AN EXPERIMENTAL EVALUATION OF UNBONDED POST-TENSIONED PRECAST ROCKING WALLS

Maryam Nazari, Graduate Student, Department of Civil, Construction and Environmental Engineering, Iowa State University, Ames, Iowa
Sri Sritharan, Wilson Engineering Professor, Department of Civil, Construction and Environmental Engineering, Iowa State University, Ames, Iowa
Sriram Aaleti, Assistant Professor, Department of Civil, Construction and Environmental Engineering, University of Alabama, Tuscaloosa, AL

ABSTRACT

While the current seismic design philosophy primarily ensures life safety in order to protect the buildings' occupants, substantial economic losses ensue when an earthquake causes structural and nonstructural damage and permanent deformations. Beginning with the PREcast Seismic Structural Systems (PRESSS) program, several researchers have investigated the use of unbonded post-tensioned rocking walls to improve the earthquake performance of buildings beyond life safety, by minimizing structural damage and residual drifts. This system consisted of a precast concrete wall attached to the foundation using unbonded post-tensioning (PT). Currently, ITG 5.2 provides design guidelines for post-tensioned precast walls based on observed behavior from several quasi-static cyclic tests. However, there is limited research done on understanding the behavior of rocking walls under dynamic loading. To address this concern, four precast concrete walls designed with unbonded PT were tested on a shake table. These experiments, conducted at 1/3.6 scale as part of the NEES Rocking wall project, used initial prestress and earthquake intensity as the main test variables. Overall, these walls satisfactorily withstood all earthquake motions, with intensities ranging from frequent to maximum considered ground motions. This paper presents the experimental observations and preliminary results including global lateral responses and critical seismic demands.

Keywords: Single Rocking Wall, Post-Tensioning, Shake Table Testing.

INTRODUCTION

Sustained operation of buildings designed to current seismic design requirements is unlikely after they are subjected to a severe ground motion. Although such well-designed structures ensure life safety for the buildings' occupants, they are prone to structural and nonstructural damage as well as experience permanent deformations as a result of allowing them to form intentional plastic hinges to help dissipate the seismic energy. The damage caused by earthquakes and subsequent economic losses underscore the need for developing seismic resilient buildings. Beginning with the PREcast Seismic Structural Systems (PRESSS) program[1] many researchers have developed and applied new technologies to improve the seismic performance of concrete structures by appreciating the idea of using unbonded prestressing. Unbonded post-tensioned precast concrete rocking wall is one of the practical examples originated from this concept to resist earthquake induced forces. This system consisted of a precast concrete wall connected to the foundation using unbonded post-tensioning (PT). Recentering feature of these rocking systems is made possible by the unbonded PTs that remain elastic up to the design drift; however, they may yield and experience some prestressing at higher seismic drifts. In addition to enabling the rocking mechanism, PTs serve as the primary reinforcement of the rocking walls and thus they should be protected against any failure. While these walls are subjected to seismic loading in real time, their rocking motion generates impact on top of the foundation, causing loss of kinetic energy and thus dissipation of energy in the form of radiation damping. This phenomenon provides a source of energy dissipation along with the inherent viscous damping of the wall.

In spite of several past investigations on this topic[1-5], dynamic rocking behavior and seismic viability of single rocking walls (SRWs) have not been investigated, and thus they are not generally favored in seismic regions. As part of an ongoing NEES Rocking Wall project, a set of shake table tests were completed on four 1/3.6 scaled specimens with different design parameters. This paper focuses on seismic response of single rocking walls subjected to ground motions with different levels of intensities. Following a comparison of test observations, influence of different design parameters on SRWs and their performance in terms of maximum permissible drifts and accelerations are presented.

TESTING OF SINGLE ROCKING WALLS (SRWs)

KEY VARIABLES

For NEES Rocking Wall project, a six story prototype precast concrete residential structure located in Los Angeles, California was designed and detailed by Nakaki Bashaw Engineering Group, Inc. This building consisted of four rocking walls; the dimensions of all four test walls were determined based on a typical wall from the prototype building. Given the payload capacity of the shake table, the test walls identified as SRW1 through SRW4 were modelled at a scale factor of 1/3.6 with dimensions of 6.25 ft. long, 16 ft. tall and 5 in. thick. Typical cross sectional details of all four test walls presented in Fig.1. The main differences between the four test walls were the amount of post-tensioning steel and the initial prestressing force. The first wall (SRW1) was designed with the amount of prestressing force to closely match the moment capacity of the prototype wall. Using SRW1 as a reference wall, SRW2, SRW3 and SRW4 were designed by varying the initial prestress force, base moment to base shear ratio and base channel at the wall base as summarized in Table 1.

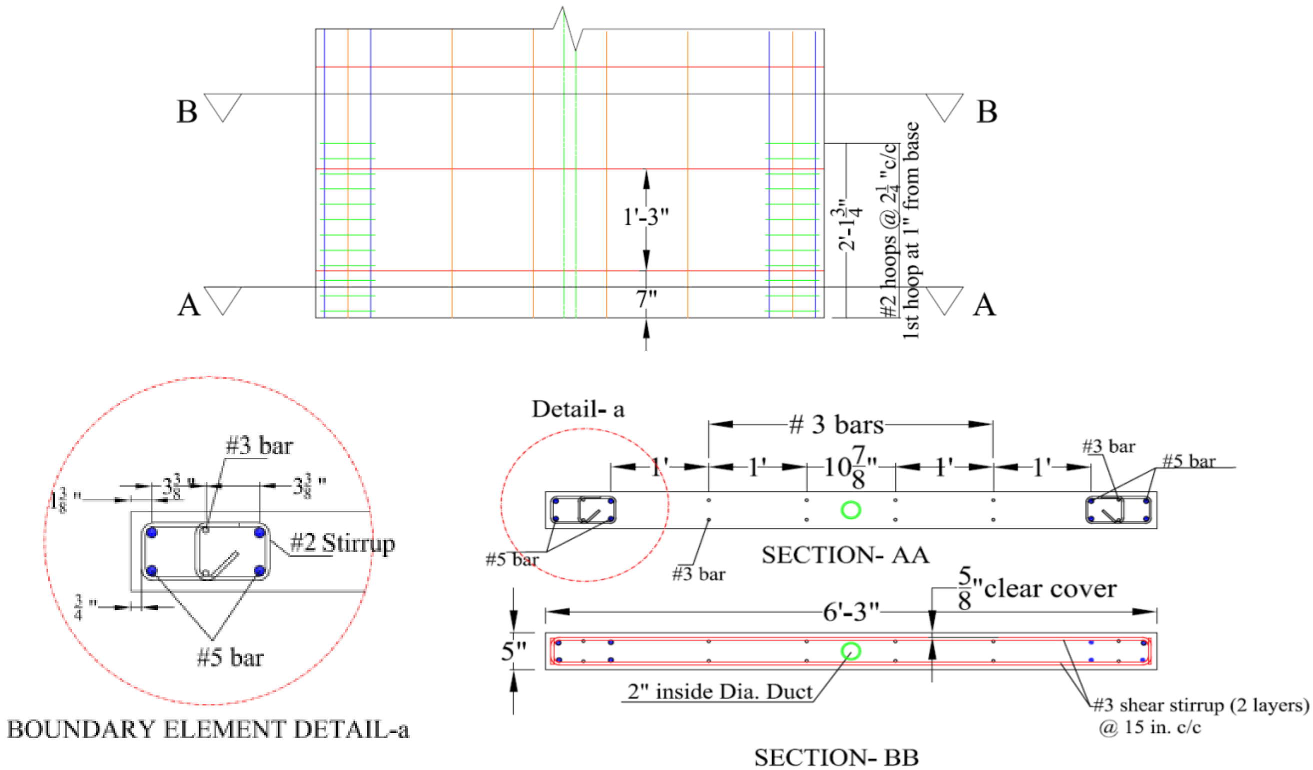

Fig. 1 Typical cross-sectional details of all four walls (SRW1-4)

Table 1 Test variables of the rocking wall specimens

Specimen	**Strand**	**Initial PT Stress (ksi)**		**Seismic Height (ft)**	**Base Channel Configuration**
		Design	**Measured**		
SRW1	4,0.5"	172.00	170.00*	14	12" @ Both Corners
SRW2	6,0.5"	172.00	148.00	14	Along the wall
SRW3	6,0.6"	172.00	170.00	14	No Channel
SRW4	6,0.6"	172.00	166.00	11.5	15" @ Both Corners

*After Test-4, PT stress dropped to 79 ksi, due to a large drift resulting from a resonance condition.

The flexural capacities of all test walls were estimated based on a simplified analysis (SA) method presented by Aaleti and Sritharan[3]. As recommended by ACI ITG-5.1 (2007)[6] and ACI ITG-5.2 (2009)[7] guidelines, all wall toes were designed with confined boundary elements so that these regions can sustain large compressive strains. To understand the value of adding steel channels at the wall base to minimize damage, different steel armoring configurations were used (see Table 1). Accordingly, no armoring was used in SRW3, armoring of the entire wall length was done in SRW2 while only the wall toe regions were armored in SRW1 and SRW4. As suggested by ITG-5 guidelines, a steel fiber reinforced grout with a specified strength of 10 ksi was used at the interface between the wall base and foundation.

SETUP

As shown in Fig. 2, the rocking walls were tested using a shake table that was attached to the laboratory strong floor using tie-downs. Seismic mass required to cause the appropriate inertia effect on these walls was estimated to be 1.67 kips-s^2/ft, which corresponded to a weight of 53.8 kips. The corresponding weight was placed on an external Mass-Rig, which was connected to the test walls using a rigid link (see Fig. 2). This arrangement modelled the appropriate inertia load, without overloading the shake table.

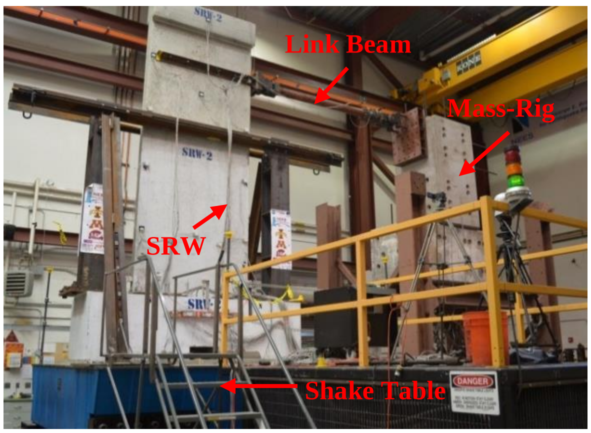

a) SRW2 on the table and mass blocks on the frame

b) Mass Blocks on Mass-Rig Frame

Fig. 2 Setup used for shake table testing

INPUT GROUND MOTIONS

Test walls were subjected to a total of 16 to 18 different input motions representing: sinusoidal harmonic excitations and two suits of recorded earthquake motions with varying intensities. In addition, the walls were subjected to white noise records and to a free vibration test at the end. In the loading protocol, white noise records, defined as very small amplitude random vibrations, are considered between applied ground motions. Maximum desired acceleration amplitudes for all white noise records are limited such that the gap opening does not occur at the base of the wall. Applying these records, initial natural frequency of the system before starting rocking motion, could be estimated. To examine the effect of duration of motion on the dynamic response of rocking specimens, the selected ground motions included four short duration motions along with six long duration motions, as summarized in Table 2. The short duration motions consisted of four spectrum compatible motions (Eq-1s to Eq-4s) as used for the pseudo dynamic testing of the PRESSS building[1], while the long duration motions were recorded ground motions in past earthquakes with appropriate scales as suggested by Rahman and Sritharan[8]. This will be further discussed in the following section .The loading history for all SRWs included three short duration spectrum compatible motions (Eq-1s, Eq-2s and Eq-3s) with increasing intensities, followed by the three long duration motions with the same intensities (IM-a, IM-b and IM-e). Between these input motions, table accelerations were maintained at zero for 30-50 seconds to let the walls complete their free vibration phase.

Table 2 List of Ground Motions with Different Intensities

Short Duration motion	**Intensity**	**Earthquake Name (Year) and Station**
Eq-1s	EQ-I	Hollister Eq. (1974); Station: Gilory #1
Eq-2s	EQ-II	San Fernando Eq. (1971); Station: Hollywood
Eq-3s	EQ-III	Imperial Valley Eq. (1940); Station: Elcentro
Eq-4s	EQ-II, III, IV	Northridge EQ. (1993); Station: Sylmar
Long Duration motion	**Intensity**	**Earthquake Name (Year) and Station**
IM-a	EQ-I	0.65* Morgan Hill EQ. (1984); Station: Gilroy #6
IM-b	EQ-II	0.64* Loma Prieta EQ. (1989); Station: Saratoga Aloha
IM-e	EQ-III	1.1* Kobe-Japan EQ. (1995) ; Station: KJM
Recent motion	EQ-I	New Zealand EQ. (2011); Station: Christchurch, REHS
Recent motion	EQ-II	Chile EQ. (2010); Station: Santiago
Used at E-Defense Test	EQ-III, IV	Kobe-Japan EQ. (1995); Station: Takatori

SCALING THE GROUND MOTIONS

Two different sets of scaling factors were considered for the input motion records. Since the testing was done at 1/3.6 scale, following the similitude, the amplitude of all motions corresponding to the full-scale walls was scaled up by the factor of 3.6 and the time step of the records was reduced by a factor 3.6. This scaling ensures that the shake table tests results would accurately emulate the seismic response of the actual prototype building. As previously mentioned, different scale factors were chosen for long duration motions to ensure the intensity of the selected earthquakes motions adequately represent frequent to maximum considered ground motions (EQ-I to EQ-IV, as presented in Table 2). More details of the scaling procedure can be found in Rahman and Sritharan[8].

RESPONSE OF WALLS

TEST OBSERVATIONS

SRW1

During the sinusoidal motions, SRW1 responded with unexpectedly large lateral displacements when a harmonic excitation with driving frequency of 1Hz and amplitude of 0.1g was applied to the test unit. Although unexpected, the high-amplitude response was later confirmed to be due to the wall reaching a resonance condition. The natural frequency of the wall (3.73 Hz) and the driving frequency (1 Hz) were not identical at the beginning of the test (0.1% drift), however, the frequency period of the rocking progressively reduced as the wall experienced rocking (1 Hz at 0.14% drift), causing the resonance response. SRW1 experienced a lateral drift of 7.3% during resonance. The observed damage to the wall corners at the end of this test are presented in Figs. 3a-c. As shown in Fig. 3a, the channel placed at the bottom of the wall experienced some bending. The PT tendons experienced yielding and thus 50% of the initial prestressing was lost. There was no further damage observed for the remainder of the test and the wall always re-centered with negligible amount of residual displacements.

During the 0.6 Kobe motion corresponding to intensity level of EQ-III, a maximum lateral drift of 3.3%, was observed while the concrete in one corner of the wall that was previously damaged during harmonic loading (see Fig. 3c) spalled off, as shown in Fig. 3d. The confined concrete still appeared to be in good condition.

For the last ground motion applied to SRW1 (Sylmar earthquake with intensity level of EQ-IV), it experienced a maximum of 14 in. relative displacement (8.4% lateral drift), with no further damage observed at the end of this test. A significant reduction in stiffness and consequently large amount of lateral displacement was observed which was suspected to be mostly due to further yielding of the post-tensioning strands. Such a large drift was not unexpected because of the loss in the initial prestress force.

SRW2

Based on the observed damage to the embedded base channels of SRW1 (see Fig. 3a), 1 in. wide soft foam pieces were placed at the ends of the wall to prevent buckling of the steel channels during impacts. The observed damage to SRW2 at the end of the testing is shown in Figs. 3e and 3f. SRW2 experienced only minimal damage due to the use of soft foam and re-centered with no residual drift after experiencing a maximum lateral drift of 5.4% when subjected to Sylmar earthquake motion (EQ-IV level intensity). A 37% drop in PT force was observed due to yielding of tendons during this test.

SRW3

SRW3 experienced a maximum of 2.63% lateral drift while it was excited by the Kobe motion, with an intensity level of EQ-IV. The observed damage to SRW3 is shown in Figs. 3g-i. During this motion, the PT strands did not experience yielding and therefore no loss of PT was observed. This test wall was designed to resist a higher base shear using greater amount of initial prestressing force. At the end of testing, three strands out of the six strands were cut to decrease the initial PT force, while initial PT stress remained as before. This was done to operate the table within the force capacity of the shake table actuator while allowing testing using higher intensity ground motions. With reduced initial PT force, under the Kobe motion with similar intensity (EQ-IV), SRW3 achieved the maximum drift of 3.1%. As presented in Fig. 3j, a large segment of the cover concrete (about 9 in. wide by 18 in. high), detached at the North West corner of the specimen, after experiencing this motion. Besides, some damage to the confined concrete was observed in the bottom 3-4 in. of the wall. The comparison of top drift time history for SRW3 before and after reducing the PT strands during the Kobe motion is shown in Fig. 4. It can be seen that SRW3 experienced more rocking with lower initial PT force and therefore experienced more damage. It is important to mention that the wall base was not armored in this case.

SRW4

Experiencing 2.28% lateral drift during the Kobe earthquake with an intensity level of EQ-IV, SRW4 satisfactorily re-centered with no damage (see Fig. 3k). Cutting three strands out of the six strands of the last single rocking wall, similar to what was described for SRW3, some damage observed at the wall base while the specimen underwent a maximum lateral drift of 5.7% during an EQ-IV intensity level of Sylmar ground motion (see Fig. 3l). It also appeared that embedding the steel channel into the base of the SRW4 significantly mitigated the observed damage compared to the unprotected rocking wall (SRW3).

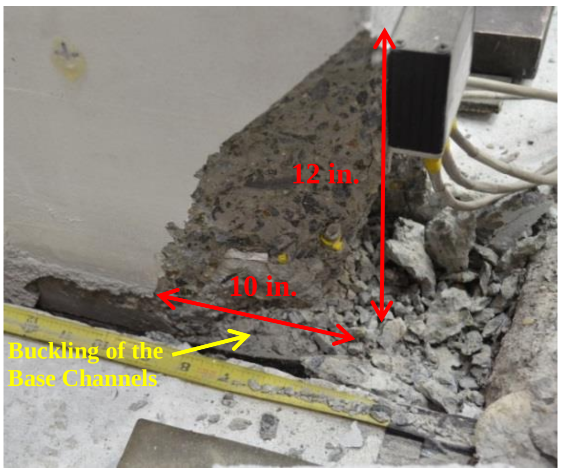

a) SRW1-Harmonic motion-SW corner


b) SRW1-Harmonic motion-NW corner

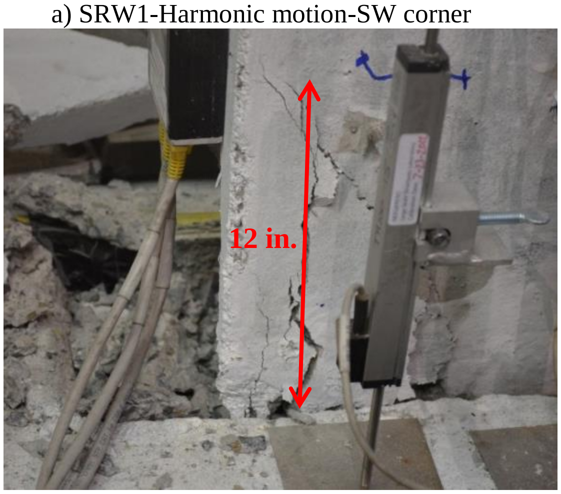

c) SRW1-Harmonic motion-SE corner

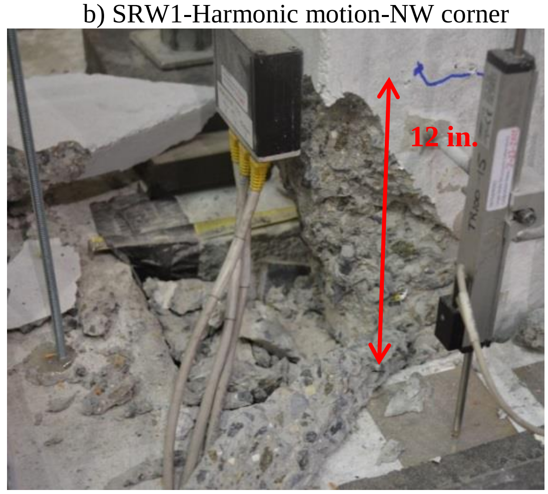

d) SRW1- SE corner (After 0.6Kobe EQ.)

e) SRW2- NW corner (End of Testing)

f) SRW2- SW corner (End of Testing)

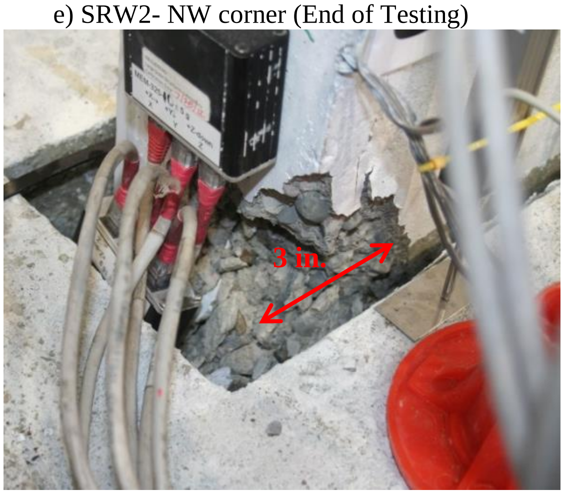

g) SRW3- SE corner (before cutting PT)

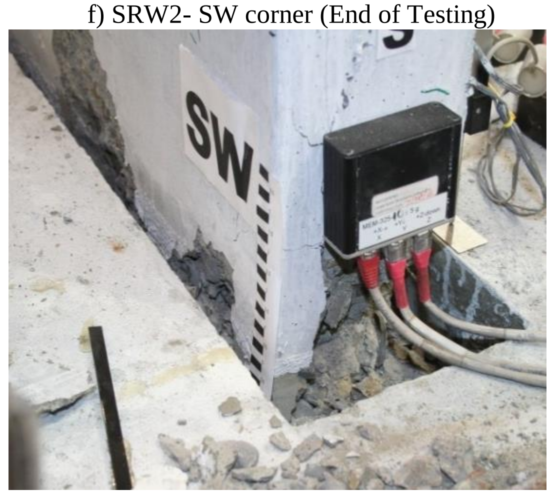

h) SRW3- SW corner (before cutting PT)

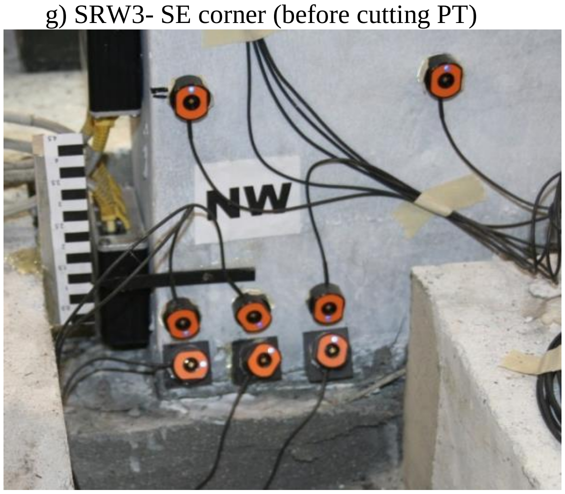

i) SRW3- NW corner (before cutting PT)

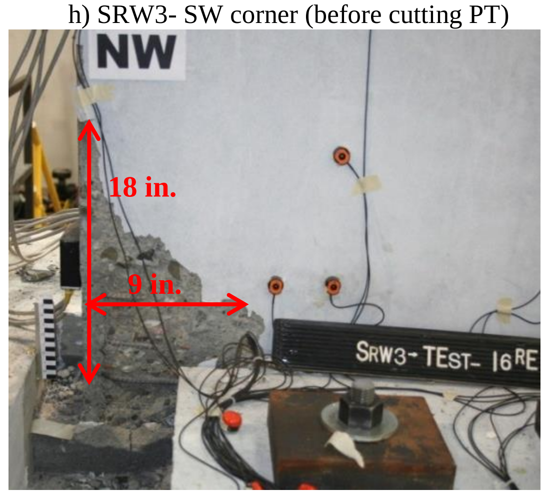

j) SRW3- NW corner (After cutting PT)

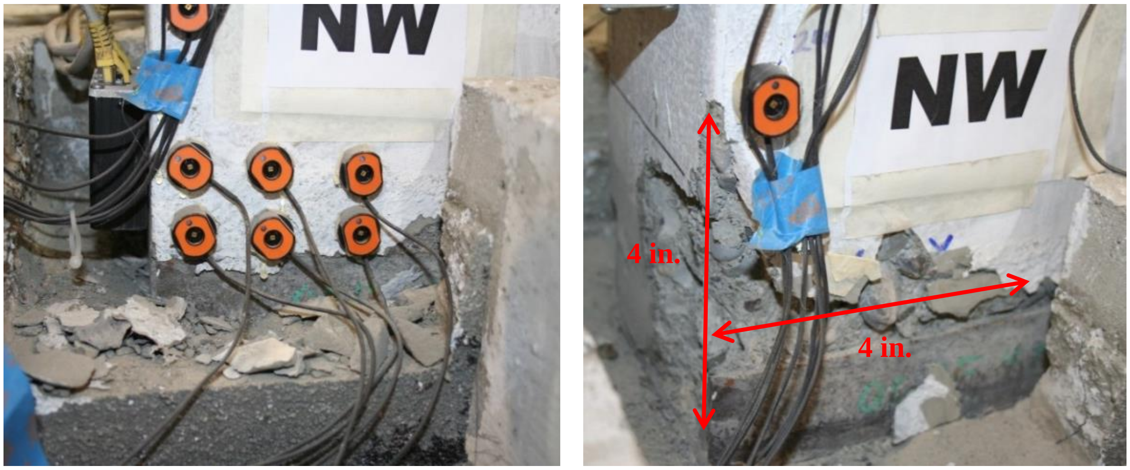

k) SRW4- NW corner (before cutting PT) l) SRW4- NW corner (After cutting PT)

Fig. 3 Experimental observations of shake table testing of rocking walls

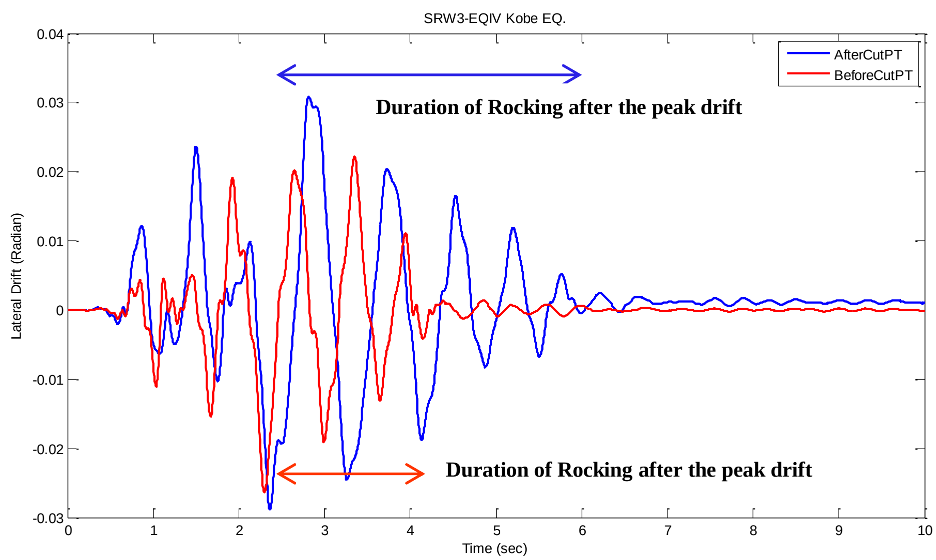

Fig. 4 Drift time history response of SRW3 with different initial PT force-Kobe EQ.

Summary

Overall, no significant damage to the rocking walls was observed during seismic testing to EQ-I and EQ-II intensity motions. Armoring the wall base with steel channels appeared to have protected the walls from experiencing any damage during the design-level (with intensity of EQ-III) and maximum considered earthquake excitations (with intensity of EQ-IV). Although some damage was observed for the unprotected toes of walls with no armoring, the damage was mostly confined to cover concrete. All walls exhibited re-centering behavior even after being excited by the maximum intensity ground motions.

EVALUATION OF EXPERIMENTAL DATA

While the experimental observations indicate considerable advantages of using self-centering rocking walls, it was also observed that some walls experienced large lateral drifts during intense ground motions. Therefore, a study based on the experimental data was conducted in this section to investigate the lateral resisting performance of four single rocking walls with different design parameters, while they were subjected to motions with different levels of intensities. In addition, critical wall demands presented for a number of test runs and compared with the acceptable limits outlined based on recommendations given in the SEAOC blue book[9, 10].

Lateral Resisting Behavior of Single Rocking Walls

To identify the seismic performance of single rocking walls, Kurama et al.[5] specified four states for the lateral resistance force-displacement response. The linear part of the rocking behavior includes the decompression state, the point where the gap opening is initiated at the wall base and continues till the point of softening where inelastic strains and spalling of cover concrete take place in the wall toe. After a significant reduction in the lateral stiffness at this level, wall rocks to higher values of lateral drift and unbonded PTs elongate and possibly reaches the yielding state of post-tensioning strands. Finally, the ultimate state of rocking behavior causes concrete crushing at wall corners. It was of interest to study the global performance of four rocking specimens with different design parameters in terms of investigating their lateral load resistance (base shear vs. lateral drift) during four levels of earthquake intensities.

<u>EQ-I intensity level motions</u>: All rocking wall specimens performed satisfactorily during small intensity earthquake loads. As noted before, the initial PT force in the SRW1 was considerably reduced due to yielding of the unbonded tendons in SRW1, after the specimen was excited by a harmonic motion to the resonance level. This reduced the initial stiffness of the wall and therefore resulted in increased amount of drift (see Fig. 5a) during the EQ-I level motions. As presented in Fig. 5b for SRW2, longer duration motions (IM-a) resulted in larger amount of drift compared to the similar intensity short duration motions (Eq1s). As shown in this figure, both of these small intensity motions (Eq1s and IM-a with intensity level of EQ-I) were repeated after exciting the specimen with higher intensity ground motions. The fourth run of IM-a motion, (shown as IMa-R4 in Fig. 5b) was applied to the test wall which was previously subjected to a very strong motion and had lost about 35% of initial prestressing. To examine the influence of initial prestressing on the response of single rocking walls, the lateral force-drift response envelope of SRW2 excited by IMa-R4 idealized with bilinear trend and compared with the case that this specimen initiated rocking with higher level of prestressing (shown with orange and blue arrows accordingly in Fig. 5b). This figure indicates that as the PT force reduces, the rocking wall has less resistance to uplift and therefore starts to rock at smaller drifts which resulted in softening of the rocking wall at smaller drifts. Also a significant reduction in the shear capacity and increase in the lateral displacement capacity of the wall could be observed in this plot. Due to equilibrium of forces, the lower the PT force, the smaller the resultant compressive force at the wall base,

which results in reduced base shear capacity. On the other hand, lower amount of this compressive force causes the wall to initiate crushing at larger lateral drifts, therefore leads to larger amount of displacement capacity. This increase in the drift capacity may also happen since the lower level of the prestress leads to larger gap opening width at the foundation interface joint (and therefore a larger lateral drift) before the tendons reach their yield state. Rocking specimens with higher initial prestressing stress (SRW3 and SRW4) linearly responded with small amount of drift during the EQ-I level tests.

<u>EQ-II intensity level motions</u>: Looking at Figs. 5c-d, it can be observed that SRW1 and SRW2 experienced a nonlinear hysteresis behavior while they were excited by an EQ-II intensity motion. Experimental results show small amount of hysteretic energy dissipation which is mostly attributable to spalling of cover concrete in the wall toe. As shown in Fig. 5c, PT tendons slightly yielded while SRW1 experienced higher lateral drift during the Sylmar earthquake motion and therefore resulted in higher amount of energy dissipation for this test wall. No significant nonlinear response was observed for SRW3 and SRW4 during the EQ-II level tests.

<u>EQ-III intensity level motions</u>: As presented in Figs. 5e-h, all the specimens demonstrated a nonlinear elastic behavior after experiencing design level ground motions with intensity of EQ-III. As shown in Fig. 5f, a 10% drop of PT force in SRW2 during the Kobe motion resulted in earlier softening of the rocking specimen, but did not affected the wall ultimate capacity.

<u>EQ-IV intensity level motions</u>: Further yielding of the post-tensioning strands dropped the PT force after the wall experienced about 4% drift (see Fig. 5i). This situation caused a significant reduction in the stiffness leading to the wall free rocking up to 8.4% lateral drift. It is interesting to mention that although the response deviated from a nonlinear elastic hysteresis behavior, residual displacement at the end of this test was noticeably below the limit Outlined by SEAOC[9]. As shown in Fig. 5j, a large lateral drift caused yielding and subsequent loss of initial prestress in the unbonded tendons and therefore low amount of energy dissipation for SRW2, when it was excited by the Sylmar motion. To study the effects of reducing the area of PT steel, while maintaining the initial stress, the lateral load response of SRW3 to EQ-IV Kobe motion were compared before and after cutting the strands in Fig. 5k. It can be observed that reducing PT area did not affect the maximum displacement drift, since the level of initial PT stress was constant and therefore similar amount of gap opening occurred for both cases to yield the PT strands. However, lowering of PT force after cutting three strands resulted in significantly smaller base shear capacity. As shown in Fig. 5l, a slight drop in PT force was observed while SRW4 underwent EQ-IV intensity Kobe and Sylmar motions, after cutting three strands

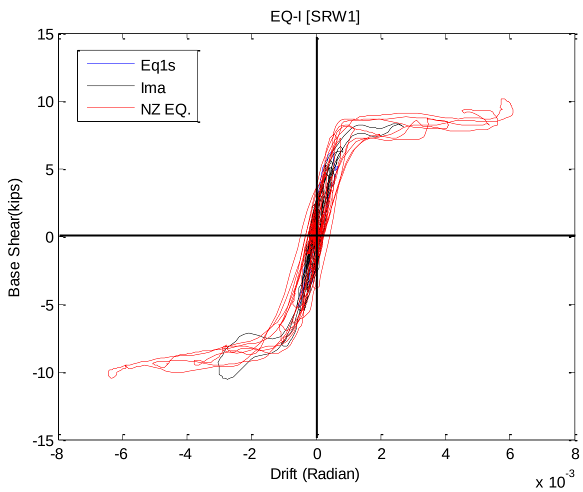

a) SRW1 (EQ-I intesity motions)

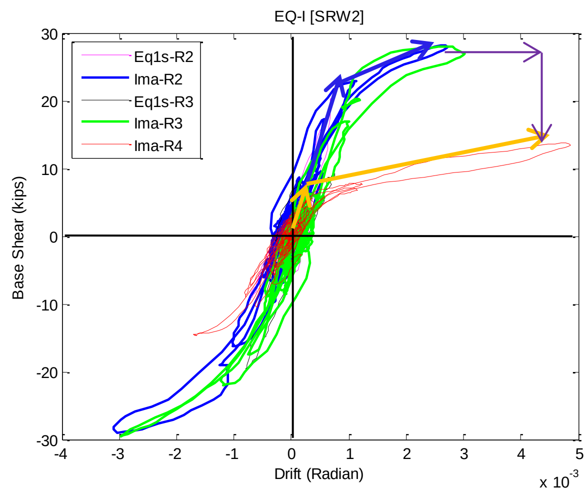

b) SRW2 (EQ-I intesity motions)

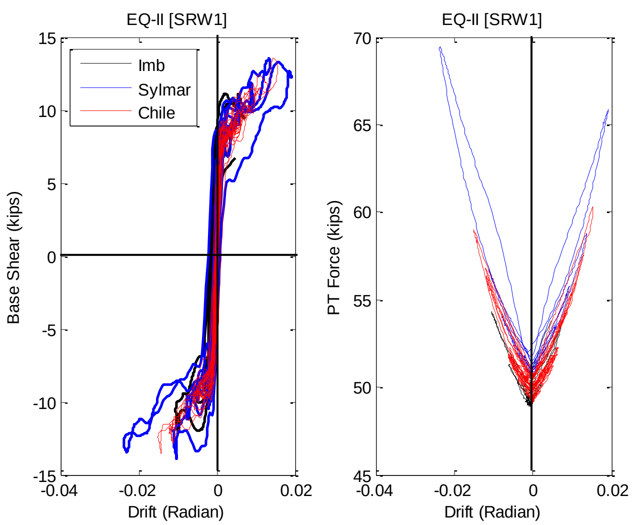

c) SRW1 (EQ-II intesity motions)

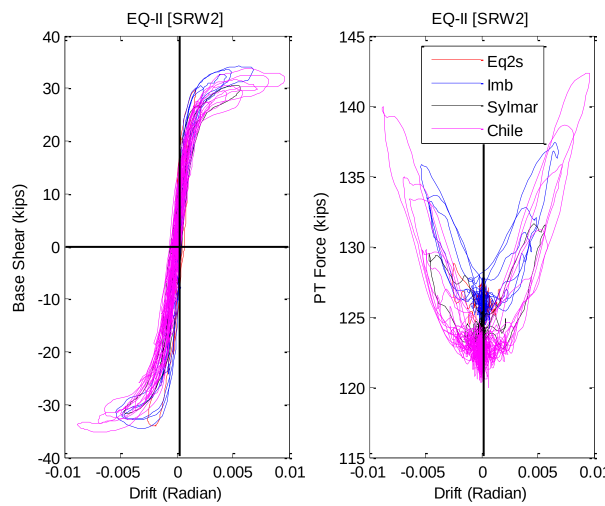

d) SRW2 (EQ-II intesity motions)

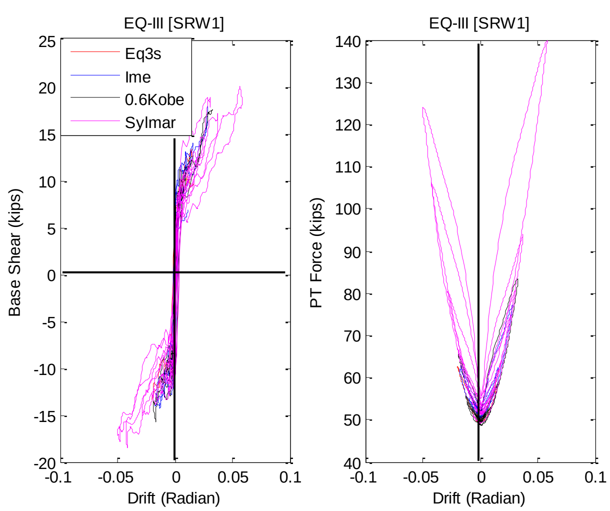

e) SRW1 (EQ-III intesity motions)

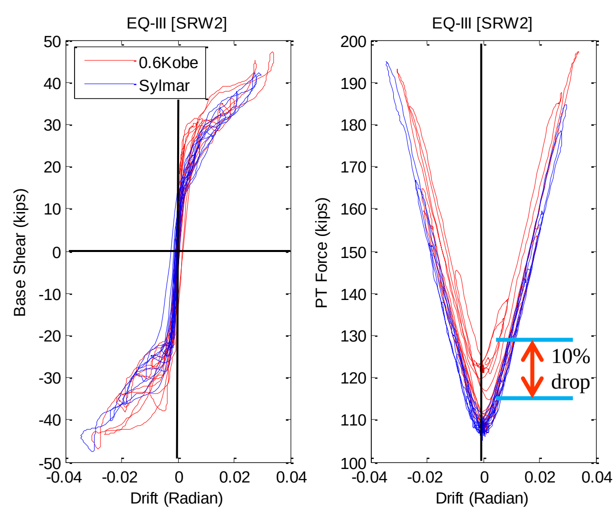

f) SRW2 (EQ-III intesity motions)

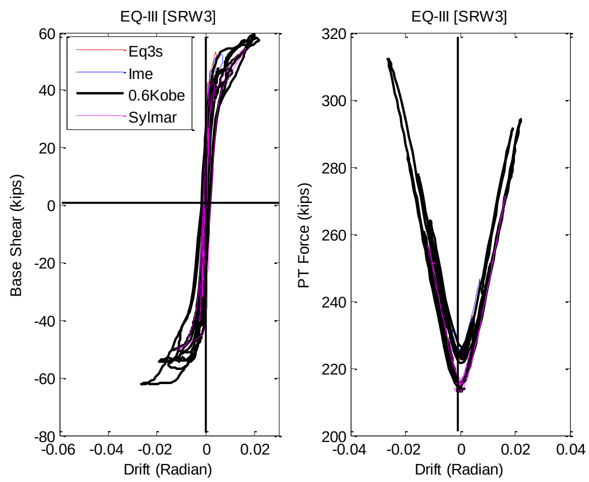

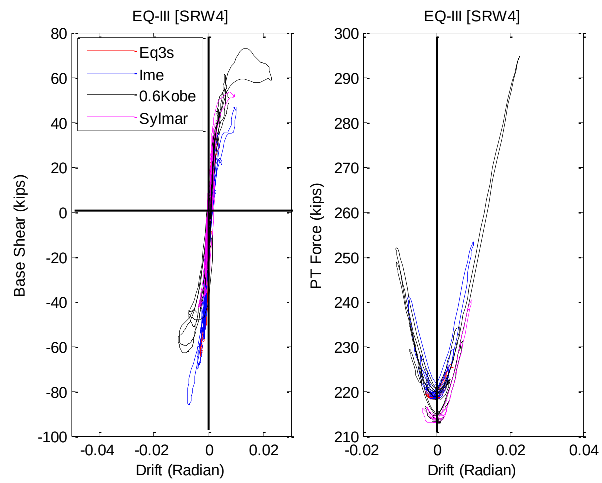

g) SRW3 (EQ-III intesity motions) h) SRW4 (EQ-III intesity motions)

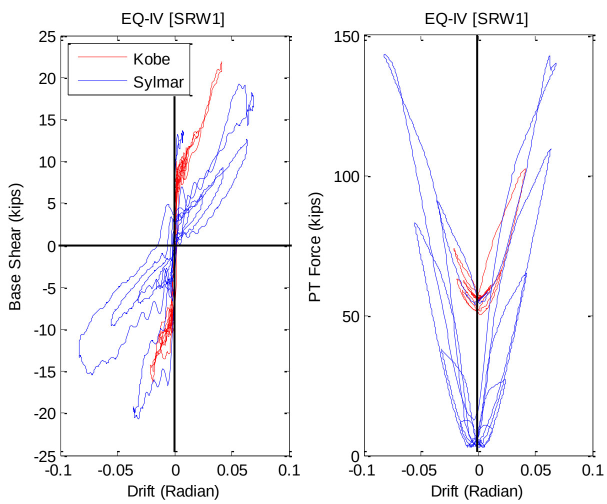

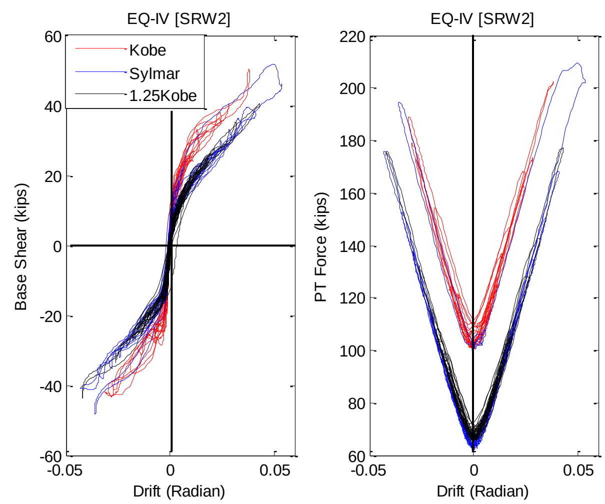

i) SRW1 (EQ-IV intesity motions) j) SRW2 (EQ-IV intesity motions)

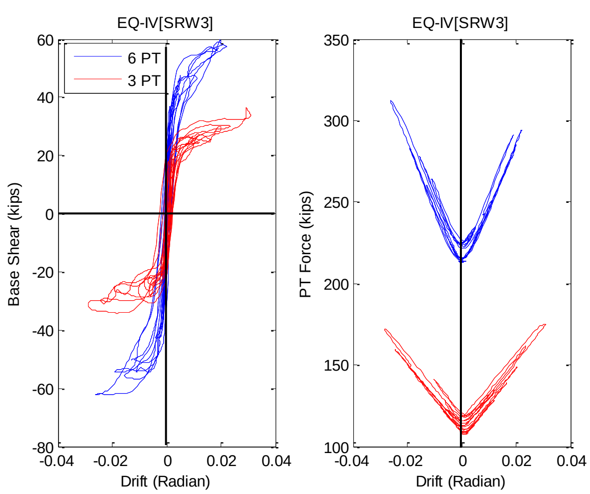

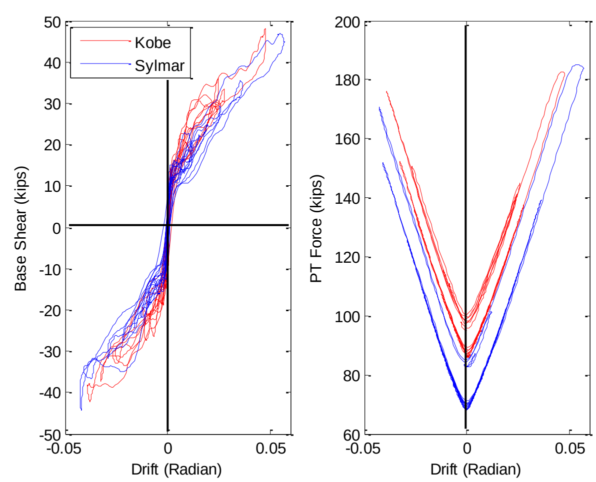

k) SRW3 (EQ-IV intesity motions) l) SRW4, with 3 strands (EQ-IV intesity motions)

Fig. 5 Lateral resisting behavior of single rocking walls

Critical Seismic Demands of Single Rocking Walls

To evaluate the performance of single rocking wall system at the four earthquake intensity levels, the critical seismic demands, in terms of the maximum lateral drift, absolute acceleration and residual drift compared with the following acceptable limits for all test runs of each specimen. According to the guidance given in the SEAOC Blue Book (Seismology Committee 1999), maximum permissible transient drifts of 0.4% (EQ-I), 1.2% (EQ-II), 2.0% (EQ-III) and 3.0% (EQ-IV); and maximum permissible residual drifts of 0.1% (EQ-I), 0.3% (EQ-II), 0.5% (EQ-III) and 0.75% (EQ-IV) were chosen as suggested by Rahman and Sritharan[10]. Acceleration limits also were selected based on their recommendations to control the forces required to anchor different types of non-structural elements to building floors under seismic condition[10]. Including the scale factor of 1:3.6, for four different levels of intensity motions these limits were suggested to be taken as 0.954g, 2.117g, 4.32g and 6.48g respectively[10]. Ratio of the maximum wall demand to these allowable limits for four specimens experiencing ground motion with different intensities (named as EQ-I to EQ-IV) and durations (named as short and long duration) are summarized in Figs. 6 to 11.

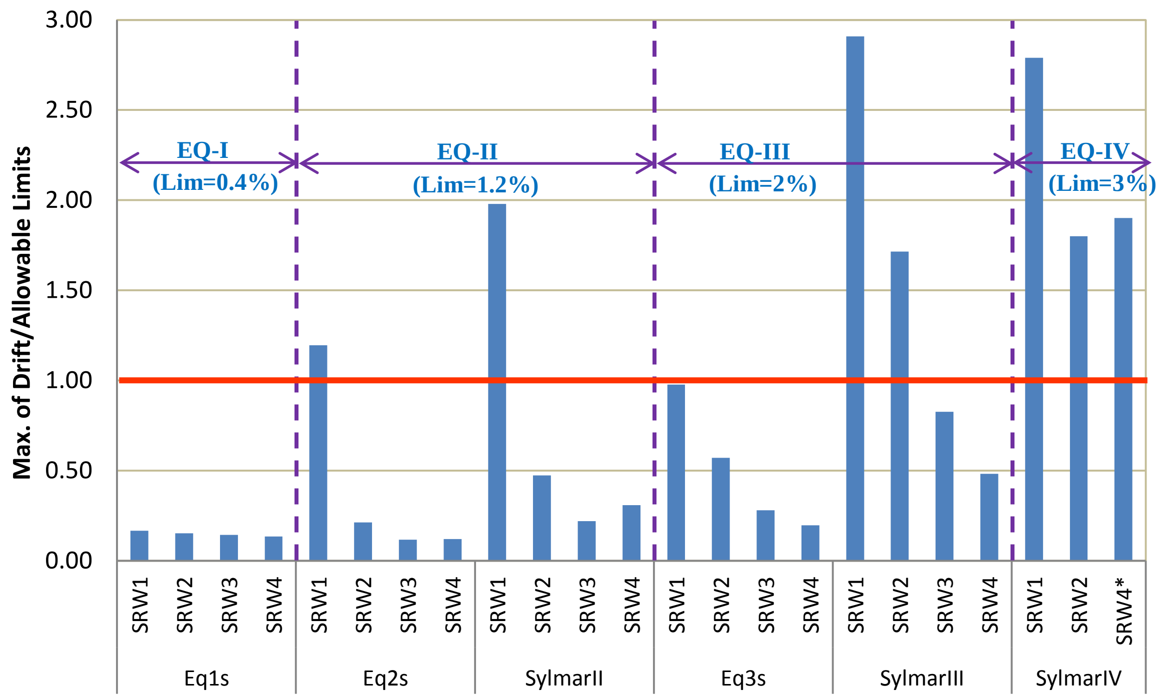

1-Sylmar #: the Sylmar motion with intensity level of #. 2- * After cutting strands (with 3, 0.6" strands)

Fig. 6 Maximum of Drift to Allowable Limits (Short Duration motions)

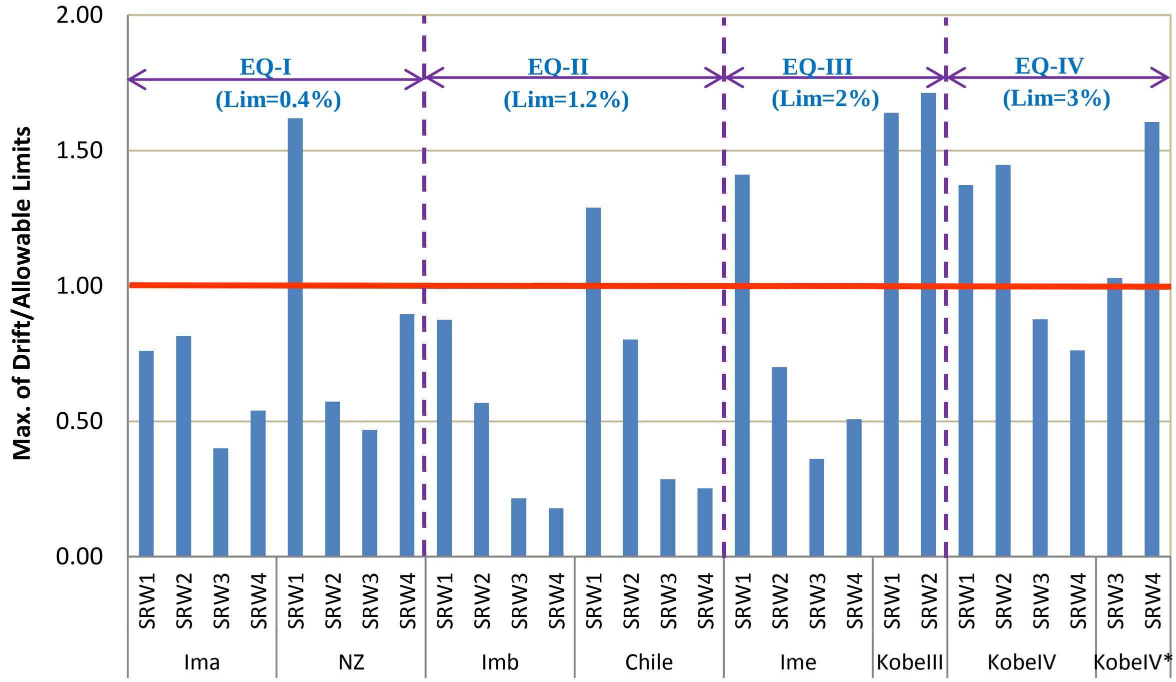

1-Kobe #: the Kobe motion with intensity level of #. 2- * After cutting strands (with 3, 0.6" strands)

Fig. 7 Maximum of Drift to Allowable Limits (Long Duration motions)

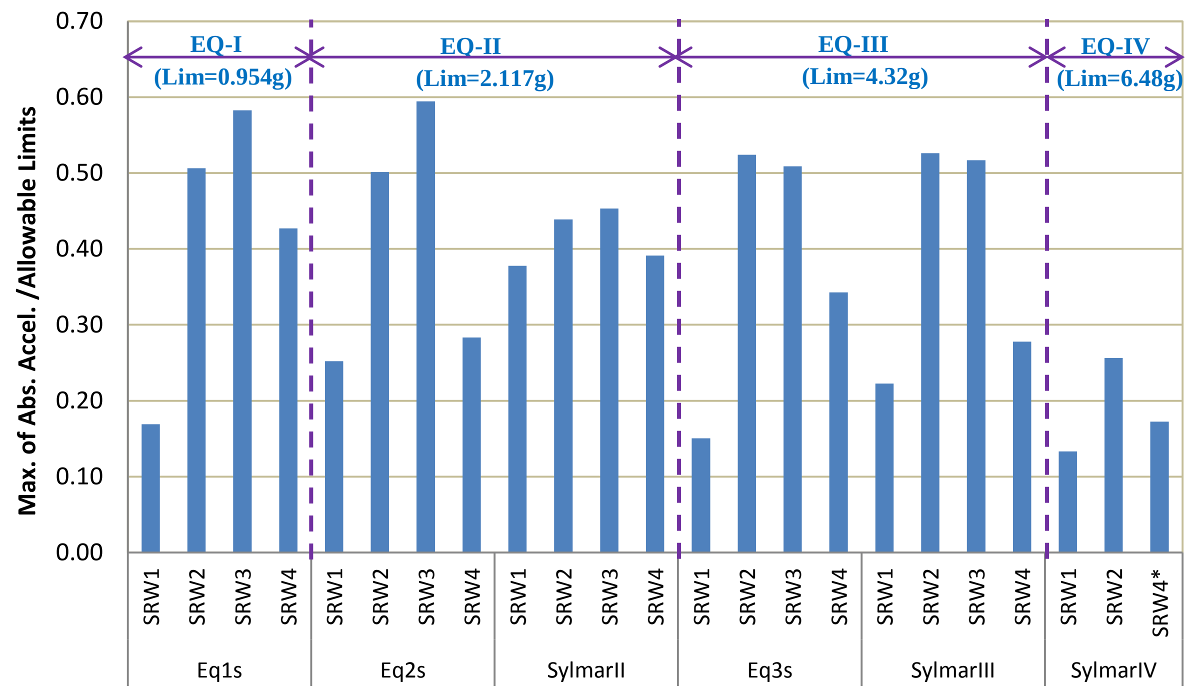

1-Sylmar #: the Sylmar motion with intensity level of #. 2- * After cutting strands (with 3, 0.6" strands)

Fig. 8 Maximum of Absolute Acceleration to Allowable Limits (Short Duration motions)

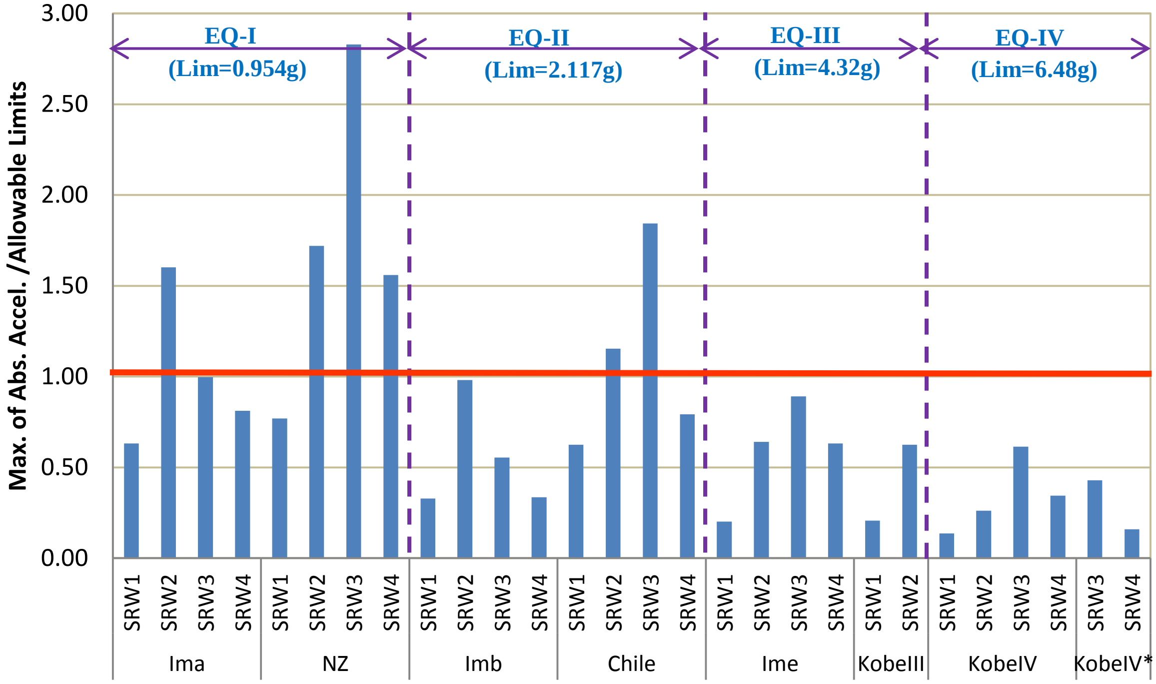

1-Kobe #: the Kobe motion with intensity level of #. 2- * After cutting strands (with 3, 0.6" strands)

Fig. 9 Maximum of Absolute Acceleration to Allowable Limits (Long Duration motions)

As presented in Figs. 6 and 7, for the EQ-I and EQ-II intensity level motions, rocking specimens performed well within the allowable limits in terms of maximum drift. However SRW3 and SRW4 with higher amount of initial prestressing had stronger tendency to achieve the maximum lateral drift less than the acceptable limits. This phenomenon was more pronounced when test walls excited by stronger motions with intensity of EQ-III and EQ-IV. On the other hand, test units underwent reduced drifts, experienced higher maximum absolute accelerations (see Figs. 6-9). In terms of dependency of response to type of motions, it can be noticed that the maximum acceleration demand of all rocking walls for all short duration ground motions were smaller compared to the same intensity longer duration motion with the same intensities (see Figs. 8-9). Also as can be observed in Fig. 9, the maximum absolute acceleration is dependent on the frequency content of the ground motion. For example, Chile and New Zealand ground motions with increased content of high-frequency cycles, forced the rocking wall to accelerate with a higher rate compared to the other motions with the same intensity. As indicated in Figs. 10 and 11, all the specimens satisfactorily self-centered with negligible residual drift.

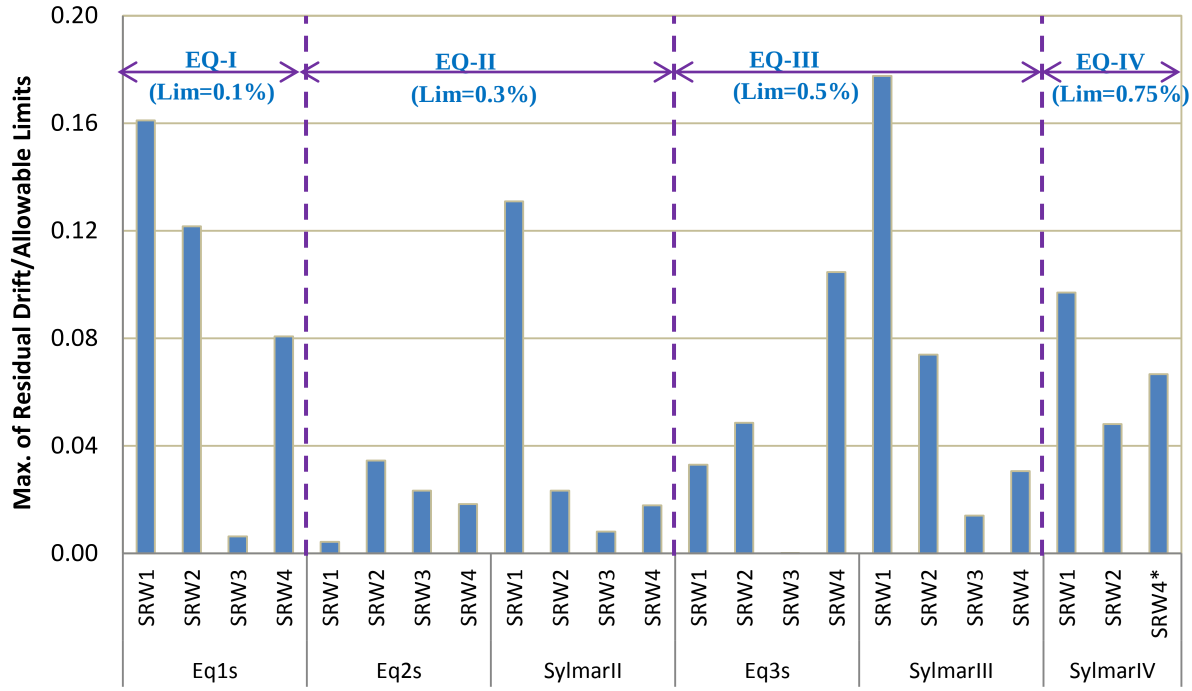

1-Sylmar #: the Sylmar motion with intensity level of #. 2- * After cutting strands (with 3, 0.6" strands)

Fig. 10 Maximum of Residual Drift to Allowable Limits (Short Duration motions)

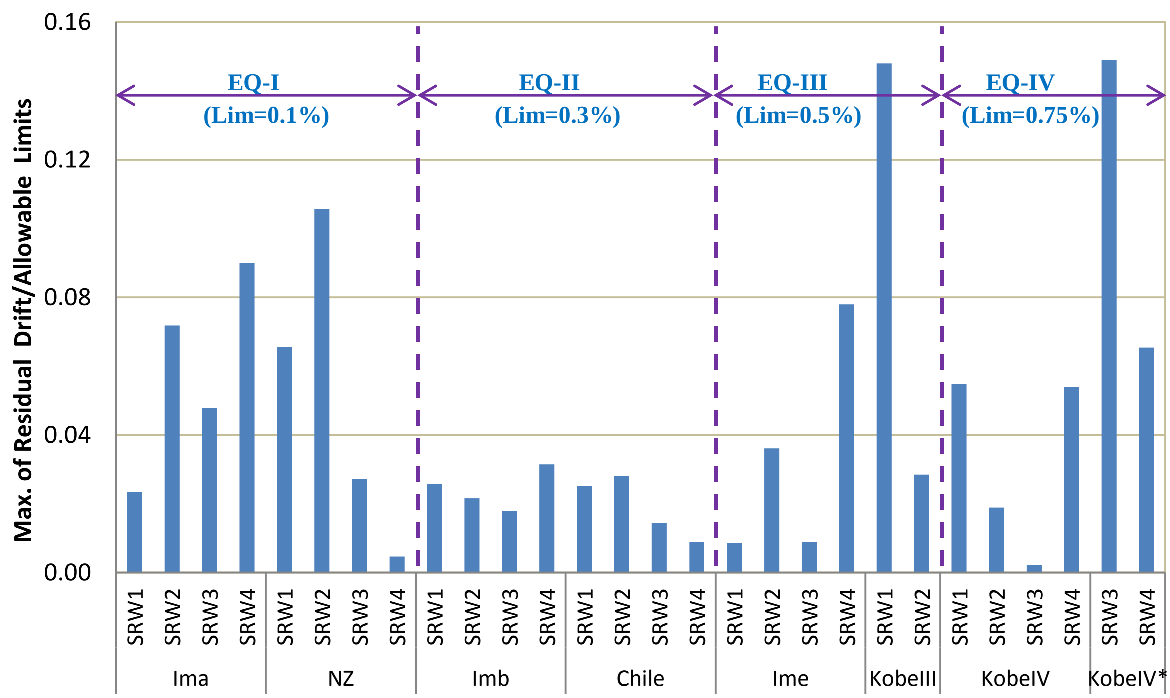

1-Kobe #: the Kobe motion with intensity level of #. 2- * After cutting strands (with 3, 0.6" strands)

Fig. 11 Maximum of Residual Drift to Allowable Limits (Long Duration motions)

CONCLUSIONS

Seismic performances of four single rocking walls (SRWs) representing a typical wall from a six story prototype building at 1/3.6 scale were first evaluated in this paper in terms of the observed damage. Then, lateral resistance performance of all SRWs with different design parameters as well as their critical seismic demands were compared using the responses recorded under different intensity level ground motions. All single rocking wall units performed well in terms of reducing both the structural damage and residual displacement at the end of different seismic hazard levels EQ-I to EQ-IV, although the maximum drift exceeded the allowable limits established based on design codes (SEAOC), particularly when they underwent design level (with intensity of EQ-III) and maximum considered earthquake excitations (with intensity of EQ-IV). Acceleration responses were mostly below the acceptable limits, except for the motions with increased content of high-frequency cycles. Comparing all the test walls, it can be noticed that decreasing initial PT stress (SRW1 and SRW2 compared to SRW3 and SRW4), the rocking walls experienced less amount of maximum accelerations; however they experienced larger drift values.

ACKNOWLEDGMENTS

The study reported in this paper was conducted as part of an ongoing National Science Foundation grant NEESR-CR: Unbonded Post-Tensioned Rocking Walls for Seismic Resilient Structures (grant No. CMMI-1041650). All shake table tests were conducted using the NEES facilities at the Large-Scale Structures Lab at the University of Nevada, Reno (UNR).

REFERENCES

1.Priestley, M. J. N., Sritharan, S., Conley, J., and Pampanin, S., "Preliminary Test Results from the PRESSS 5-Story Precast Concrete Building", *PCI Journal*, V. 44, No. 6, 2000.
2. Perez, F. J., Pessiki, S., and Sause R., "Seismic Design of Unbonded Post-Tensioned Precast Concrete Walls with Vertical Joint Connectors", *PCI Journal*, V. 49, No. 1, Jan-Feb. 2004.
3. Aaleti, S., and Sritharan, S., "A simplified analysis method for characterizing unbonded post-tensioned precast wall systems", *Journal of Engineering Structures*, V. 31, Aug. 2009, pp. 2966-2975.
4. Rahman, A., and Restrepo, J.I., "Earthquake Resistant Precast Concrete Buildings: Seismic Performance of Cantilever Walls Prestressed using Unbonded Tendons", *Research Report 2000-5, Department of Civil Engineering, University of Canterbury, Christchurch, New Zealand*, 2000.
5. Kurama, C., Y. "Seismic Design of Partially Post-Tensioned Precast Concrete Walls" *PCI Journal*, V. 50, No. 4, July-Aug. 2005, pp. 100-125.

6. ACI Innovation Task Group 5. Acceptance criteria for special unbonded post-tensioned precast structural walls based on validation testing (ACI ITG 5.1-07) and commentary (ACI ITG R5.1-07). Farmington Hills (MI): *American Concrete Institute*, 2007.
7. ACI Innovation Task Group 5. Design of a special unbonded post-tensioned precast shear wall satisfying ACI ITG-5.1 requirements (ACI ITG 5.2-09). Farmington Hills (MI): *American Concrete Institute*, 2009.
8. Rahman, A., and Sritharan, S., "Performance-Based Seismic Evaluation of Two Five-Story Precast Concrete Hybrid Frame Buildings", *Journal of Structural Engineering*; V. 133, No. 11, Nov. 2007.
9. Seismology Committee. _1999_. Recommended lateral force requirements and commentary (Blue book), *Structural Engineers Association of California _SEAOC_, Calif.*, 327–421.
10. Rahman, A., and Sritharan, S., "An Evaluation of forced-based design vs. direct displacement-based design of jointed precast post-tensioned wall systems", *Journal of Earthquake Engineering and Engineering Vibration*; V. 5, No. 2, Dec. 2006.